IIETA International Information and Engineering Technology Association
Advancing the World of Information and Engineering

Journal Européen des Systèmes Automatisés
Vol. 56, No. 6, December, 2023, pp. 917-927
Journal homepage: http://iieta.org/journals/jesa

Hybrid Optimization for Power Quality Assessment in Hybrid Microgrids: A Focus on Harmonics and Voltage

Devika Rani Motukuri[1*], P. S. Prakash[1], M. Venu Gopala Rao[2]

[1] Department of Electrical Engineering, Faculty of Engineering & Technology, Annamalai University, Chidambaram 608002, India
[2] Department of Electrical & Electronics Engineering, QIS College of Engineering & Technology, Ongole 523272, India

Corresponding Author Email: devikamothukuri@pvpsit.ac.in

https://doi.org/10.18280/jesa.560603

Received: 16 June 2023
Revised: 20 November 2023
Accepted: 30 November 2023
Available online: 28 December 2023

Keywords:
renewable energy, harmonic distortion, hybrid microgrid, hybrid grey wolf supported sparrow search optimization algorithm, PID controller, power quality, renewable energy, voltage quality

ABSTRACT

Renewable energy's (RE) broad acceptance can be attributed to market liberalization, as well as ecological and monetary benefits. Intermittent nature of renewable energy (RE) and unpredictable load behaviour lead to voltage aberrations and harmonic distortions in interconnected hybrid microgrids (HMG).Voltage quality and the harmonic distortion are all metrics used to evaluate power quality.Efficient control approaches are required to reduce harmonic distortions and improve voltage quality for steady power transmission. This research proposes a hybrid Grey Wolf supported sparrow search optimization algorithm (GWSSSOA) method for assessing voltage quality and harmonics in a microgrid that combines renewable energy sources with conventional power generation.To maximize the microgrid's control and operation, guarantee its dependability, and lessen its impact on the grid. Hybrid microgrids can benefit greatly from GWSSSOA's use in voltage quality and harmonic distortion assessment. The goal of this research is to use the GWSSSOA technique in conjunction with the PID controller to achieve real-time optimization of the controller's settings for minimizing harmonic distortions and maintaining stable voltage across the microgrid. The efficiency of the proposed approach is measured against that of alternative optimized controllers. The recommended controller was developed in the MATLAB/Simulink environment.

1. INTRODUCTION

The broad adoption of renewable electricity (RE) is increasingly required because of the depletion of hydrocarbon-based fuel supplies and the ever-increasing demand for electricity.Because of their infrequent nature, inexhaustible sources like energy derived from the sun and wind can introduce a wide variety of power quality issues when integrated. A reliable and diminishing supply of free electricity is crucial to the progress of industrialization, urbanization, agriculture, and economic growth in any country. For the prolonged load requirement, a greater effort from traditional power sources is required to guarantee continuous power supply for all operating sectors [1]. In order to prepare for the greater influence that renewable energy integration would have, microgrids have been implemented into the current power systems [2-5]. Microgrids (MGs) are voltage-diverse, dynamic distribution networks that include multiple loads, DGSs, and operational control techniques in both isolated and interconnected topologies. Several problems with power quality (PQ) are caused by the use of power electronic devices and by variations in load. Many problems with PQ are also brought on by the various nonlinear sources present in MGs [3-6]. Issues with MGs-PQ can manifest as anything from harmonics to voltage spikes and dips to unbalance.

Standard proportional-integral-Derivative (PID) controllers are the most practical option due to their additional degree of freedom, affordability, and simplicity when compared to more advanced controllers such as the Sliding Mode Control (SMC) [7-10], the Model Predictive Controller (MPC) [8], and the H_2/H_∞ controllers [9]. Parameter tweaking of the PID controller is very important for a large, dynamic HMG model.Poor dynamic response in the system's voltage regulation might be the result of incorrect tuning of the PID parameters, which can lead to system instability [11]. To address this, numerous articles have been written about employing artificial neural networks (ANN) [12, 13] and fuzzy logic control (FLC) [14] to fine-tune the PID controller's gain values. But because the choice has no hard and fast mathematical meaning, it may, on occasion, lead to subpar controller performance.This research seeks to optimize harmonic distortion and enhance voltage regulation within a hybrid microgrid to achieve grid stability, reliability, and energy efficiency.

Rapid integration of renewable energy sources, advancements in energy storage technologies [12-16], and a growing emphasis on sustainable energy solutions are all hallmarks of the current seismic shift in the global energy landscape.In the midst of this paradigm shift, hybrid microgrids have emerged as a pivotal innovation that

embodies the future of decentralized and environmentally responsible energy generation and distribution [17]. These hybrid microgrids, which seamlessly integrate multiple power sources, including solar, wind, batteries,and conventional grid connections,hold the promise of enhanced energy self-reliance, improved resilience [18-20], and significant reductions in greenhouse gas emissions.While power quality is crucial to the safe and efficient functioning of any electrical system, the complex dynamics inside these microgrids provide new challenges [21-24].

1.1 Challenges related to power quality in hybrid microgrids

The challenges associated with power quality in hybrid microgrids are multifaceted.Due to their inherent variability, renewable energy sources like solar and wind create voltage variations, while non-linear loads and switching devices further distort electrical waveforms with harmonic distortions [25]. These power quality issues can lead to equipment damage, operational inefficiencies, and grid instability [26]. Voltage quality concerns often manifest as voltage sags, swells, and frequency variations,while harmonics manifest as distortions in the sinusoidal voltage and current waveforms, affecting both the grid-connected and off-grid components [27-30].

1.2 Research objectives and motivation for optimization-driven assessment

In this context, this research is driven by a central aim: to develop and implement optimization-driven assessment methods for mitigating voltage fluctuations and harmonics in hybrid microgrids [31]. The reasons behind this attempt are twofold. It is crucial that users have access to steady, high-quality electricity in hybrid microgrids, independent of the energy sources or operating conditions [32].

Second, the optimization-driven approach represents a compelling pathway to address power quality issues by harnessing advanced mathematical algorithms and control strategies. By adopting this approach, we seek to harmonize the complexity of modern energy systems with the precision of mathematical optimization, ultimately enhancing power quality, grid stability, and energy efficiency [33].

As we embark on this research journey, we aim to not only identify and assess power quality issues within hybrid microgrids but also to chart a course toward actionable strategies for their resolution. Significantly advancing the integration of renewable energy sources while maintaining the highest standards of power quality, this study constitutes a major contribution to the ever-changing face of energy systems.Section 2 of this paper details the literature study ,aspects of the microgrid model that will help accomplish the paper's goals explained in Section 3.In this article's fourth section, we'll focus on the fundamental block diagram of a hybrid microgrid and how its parts work together. In Section 5, hybrid shunt active power filter was introduced. In Section 6, we will analyze the effects of the hybrid Grey Wolf supported sparrow search optimization algorithm (GWSSSOA) on the PID controller's fine-tuning parameters for harmonic supression and improved voltage quality.As a part of results and conclusion, Section 7 and Section 8 presents a comparison of voltage quality at different buses and various performance indices.

2. LITERATURE STUDY

One specific example of a metaheuristic algorithm is the optimization methods presented in Table 1.

Table 1. Examination of previous research about the voltage quality and harmonic assessment

Ref. No.	Controller Type	Optimization	Model Description	Limitations
[2]	PID	GWO	Two Area System with solar and wind systems.	The most significant limitation of this optimization technique is trapping in local optimal points.
[7]	PID	GWO	Three Area System with solar,wind and disesel sources.	Poor exploration results from the GOA optimization search procedure starting with a population or flock of grasshoppers whose placements are similar to design vectors.
[6]	PID	Hybrid PSO-GSA	WTPG, STPP, BES, and thermal plants in area 2 as well as STPP, PV, SMES, and thermal power plants combining GDB and GRC in area1 and pv,wind in area2.	Its main drawback is a slow convergence rate with poor exploration ability.
[3]	PID	DE	Two-area multi-source with hydro, thermal, and wind power plants in each area.	Nonlinearities are not taken into account. DE's limitations prevent it from being used to solve many difficult real-world issues in continuous domains.
[7]	PID	WOA	Two-area reheat thermal system.	Nonlinearities are not taken into account. The drawback of WOA is that, in the later stages of WOA iteration convergence, whales are pulled to the coefficient vector; hence, the entire whale population rapidly approaches the local optimum for the high-dimensional optimization problem.
[14]	PID	HIO	Two-area reheat turbine power plant with gas and hydro units in each area.	RER has not been considered in this study.
[17]	PID	SSO	Two-area thermal system with GRC and GDB considered with the wind power plant in both the areas.	The drawback of SSO is that the update rule fails when one of the dimensions has a lower bound other than zero.

Because they are simple to use throughout the whole optimization process and have minimal requirements for function evaluation, individual algorithms are useful. Due to the significant danger of local optima stagnation, it might be difficult for individual meta-heuristic algorithms to strike a balance between exploration and exploitation in their search for the global optimum.Meta-heuristic algorithms undergo several adjustments to improve their performance in order to address this problem [34-36]. Applying chaos theory to meta-heuristic algorithms is one of the newest and most well-liked techniques for increasing the exploration/exploitation and global convergence speed of optimization algorithms, leading to a wider range of possible solutions [37]. A second method is to combine two algorithms. Later in the convergence process, however, SSA is vulnerable to local optima because of insufficient exploration [38]. These problems have an indirect effect on SSA's optimization power, making it impossible to find the best possible global solution.

The benefits and drawbacks of each algorithm suggest that a hybrid approach may be the best way to eliminate the drawbacks and get the benefits of both SSA and GWO. In an effort to improve the controller's performance in terms of steady-state and dynamic reactions to voltage and harmonics fluctuations and power flow in linked power systems, the new methodology is integrated by two differenr optimization techniques.

The following is a brief overview of the present research most important findings:

1. The SSA algorithm's exploitation potential is enhanced with the suggested hybrid GWSSSOA algorithm, and the algorithm's efficacy is demonstrated versus other algorithms via testing on a number of classical benchmark functions.
2. Harmonic and voltage quality assessments in an MG network with power from renewable sources integration involves working with an automatically tuned controller.
3. A real-world solar power plant's data is used to test the suggested technology under variable and critical conditions.
4. The proposed method's effectiveness and durability are explained through various voltage quality indices and harmonic assessment.

3. THE CONCEPTUAL FRAMEWORK FOR THE PLANNED APPROACH

3.1 Layout of the microgrid and its parts

3.1.1 Role of various microgrid components

In this part, we describe the suggested three-stage paradigm in great detail. MATLAB/Simulink R2019a was used to run simulations of the final model. Detailed model is developed to help understand the dynamics of MG in different operating circumstances. The creation of a model of MG and the details of its constituent parts are as follows:

Solar Module: Photovoltaic (PV) panels, often referred to as solar panels, play a crucial role in a microgrid, contributing to the system's resilience, sustainability, and ability to generate and store electricity [39]. As a renewable energy source, solar power can lessen the microgrid's impact on the environment. The solar panel's specifications are displayed in Table 2.

Wind Turbine: Wind turbines play a crucial role in a microgrid by harnessing wind energy and converting it into electricity. The microgrid's reliance on a single energy source can be decreased by incorporating wind turbines using alternative green energy methods. The wind turbine specifications are displayed in Table 3.

Battery: Batteries play a critical role in a microgrid by providing energy storage, enhancing system reliability, and enabling efficient utilization of renewable energy sources. Batteries may offset the unpredictable nature of alternative energy resources by storing surplus energy and releasing it whenever the sources fail to generate power. The Battery specifications are displayed in Table 4.

Loads: The stability of the proposed microgrid design is tested by subjecting it to nonlinear and unbalanced loads. The features of proposed filter have been fine-tuned to ensure optimal operation across a wide variety of conditions. The battery, DC link, and switches with antiparallel diodes are modelled in the design to eliminate harmonics.

Table 2. Model of solar panel: 1SOLTECH1 1STH-230-P

Num	Measure	Values
1	Power maximum value	228.735W
2	No of cells	60
3	Open ckt voltage	29.9V
4	Short ckt current	8.18A
5	Peak power voltage	29.9V
6	Peak power current	7.65A
7	Irradiance	1000
8	Frequency	50Hz

Table 3. Dimensions of wind generators

Num	Measure	Values
1	Initial wind velocity	12m/s
2	Initial angular velocity	0.4m/s
3	Maximum elevation angle	45 deg
4	Maximum rate of change of pitch angle	2 deg/s
5	Universal Bridge	

Table 4. Battery parameters

Num	Measure	Values
1	Battery response time	30 Sec
2	Nominal voltage	1.5 V
3	Original charge status	100%
4	Group	NIMH batteries
5	Rated capacity	6.5 Ah

3.1.2 Importance and potential challenges of various Microgrid components

Despite the issues of intermittency, fluctuation, and the necessity for energy storage to provide a steady power supply, the selected microgrid components provide energy from renewable sources, reducing dependency on fossil fuels and minimizing greenhouse gas emissions. Batteries store excess energy for later use, enhance reliability, and improve grid stability besides the challenges as cost, efficiency, lifespan, and disposal of batteries, as well as matching storage capacity with demand.

In view of load management and control systems, continuous energy consumption needs to be regulated; critical loads prioritization is possible with complex control algorithms and interoperability of diverse components leads to voltage quality challenges [40]. For reliability and energy autonomy, microgrids can operate in both grid-connected and island modes, however this integration of power electronic converters presents significant hurdles in the form of harmonic distortion and synchronization. Each component in a

microgrid contributes to the systems overall functionality, sustainability, and resilience. Successfully addressing the major challenges such as voltage quality issues and harmonics associated with these components is essential for building efficient and reliable microgrid systems.

3.2 Importance of chosen optimized PID controller

Using nonlinear and unbalanced loads as examples, we illustrate how a PID controller and a proposed controller may reduce total harmonic distortion (THD) with greater efficiency than either a filter that is passive (PF) or a power filter with active filtering (APF). The most important result of this research is that: improvement in voltage quality indices and reduced harmonic distortion at various critical buses. Figure 1 shows the controller's detailed design. The DG includes solar panels, wind generators, and batteries to store energy. Excess power can be stored in batteries and used to reduce demand at a later time. To successfully handle the PQ problems, minimize the THD, and enhance the voltage regulation, a novel PID controller with improved performance is offered, and a hybrid metaheuristic approach called GWSSSOA is developed to provide the most ideal signal for the controller.

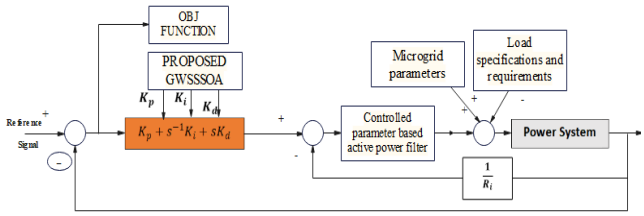

Figure 1. PID controller tuning as per objectives

3.3 Technical details of filter and its connection to grid

It was suggested to employ VSI in order to enhance the functioning of active power filters. Figure 2 shows a technical drawing of a redesigned APF (active power filter) that relates to this particular research. A redesigned power filter consists of an uncontrolled rectifier, an inverter fed with a voltage source, and a filter made up of passive components. The redesigned power filter regulates the magnitude of the nonlinear load's harmonic components.

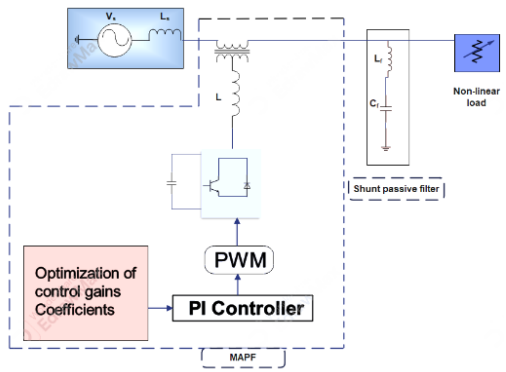

Figure 2. Technical configuration of filter and its integration with the grid

PCC uses a voltage source converter to supply compensating current, reducing the negative impacts of harmonics. To mitigate harmonics and protect the PWM converter's power limit, the system incorporates both active and passive filters. PWM converter production costs can be decreased by using power MOSFETs in place of more costly components. Power quality (PQ) in a distribution system can be improved by eliminating harmonics at the power factor correction (PFC) by injecting harmonic current of equal and opposite amplitude

4. MATHEMATICAL MODELLING OF THE PROPOSED MODEL

4.1 Step by step illustration of overall model

A photovoltaic system consists of four basic components: sunlight, a diode parallel resistor (representing leakage current), a series resistor, and a power supply. Voltage-current specific equation of a solar cell is:

$$I_{pv} = I_{ph} - I_s\left[exp^{\left(q(V_{pv}+I_{pv}R_s)/kt\right)} - 1\right] - \frac{v_{pv}+I_{pv}r_s}{R_p} \quad (1)$$

The photocurrent primarily relies on the cell's operational temperature and radiation from the sun.

$$I_{pv} = \frac{[I_{SC}+K_I(T_C-T_{Ref})\lambda]}{1000} \quad (2)$$

The saturation current varies with the cell's temperature.

$$I_S = I_{RS}(T_C/T_{Ref})^3 e^{\left[\frac{qE_G(1/T_{Ref}-1/T_C)}{kA}\right]} \quad (3)$$

Two of the most crucial indicators of cell electrical performance are the open-circuit voltage v_{oc} and the short-circuit current I_{sc}. Any of these improvements can be applied to any sufficiently complex design for a PV solar cell as:

$$I_{PV} = I_{PH} - I_S\left[e^{\left(\frac{q(V_{PV}+I_{PV}R_S)}{kT_CA}\right)} - 1\right] \quad (4)$$

It is possible to think of the battery as a nonlinear voltage source [26], with an output voltage that depends on both the current and the battery's state of charge (SOC). Two values identify the battery's terminal voltage and charge level.

$$V_b = V_O + R_b i_b - K\frac{Q}{Q-\int i_b dt} + A * e^{(B\int i_b dt)} \quad (5)$$

The non-linear component within the standard Shepherd framework is equal to:

$$soc = 100\left(1 + \frac{\int ibdt}{Q}\right) \quad (6)$$

This indicates a voltage whose shape is not linear with respect to either the magnitude of the current or the state of charge of the battery. Therefore, the battery's voltage will be close to zero when it has been completely discharged and no current is flowing. The voltage suddenly drops as soon as the current begins to flow again. This model is both effective and representative, as it produces realistic battery behavior.

The speed with which a particular volume of air is moving during a given period of time can be expressed as its kinetic

energy [28]. Then, we may write out the equation for the wind's potential energy as:

$$P_{air} = \frac{1}{2}\rho A V^3 \tag{7}$$

$$P_{wind\ turbine} = C_p \times P_{air} \tag{8}$$

In Eq. (7), power coefficient C_p, which decreases the amount of power delivered to the rotor of a wind turbine, characterizes the available wind power.as shown in Eq. (8).

If a turbine can extract no more than 59.3 percent of the power from an air stream, then that point is the upper constraint on C_p, as defined by the Betz limit. Rotor blades for wind turbines typically have C_p values between 25% and 45%.

4.2 Overview of mathematical modeling to test proposed controller performance

We suggest a set of x harmonics, where n is any integer from 1 to N. Components, including current I(t) and voltage $V_s(t)$, are located in the same place, and their relationships are given by the Eq. (9) through (7) below relates the mathematical model of the controller:

$$V_s(t) = \begin{bmatrix} V_{S1} \\ V_{S2} \\ V_{S3} \end{bmatrix} = \begin{bmatrix} \sum_{x=1}^{N} V_{sn1} \sin(\mathrm{x}(\omega \mathrm{t})) \\ \sum_{x=1}^{N} V_{sn2}\, sin(x(\omega t - 120°)) \\ \sum_{x=1}^{N} V_{sn3} sin(x(\omega t - 240°)) \end{bmatrix} \tag{9}$$

Using the Eqs. (10) to (15) below with an elevated power factor, the compensatory power from the grid P_S should be near to the real power given by the grid P_S.

$$P_S = P_L + P_l - P = \frac{3}{2} V_{S1} \tag{10}$$

(I_{Ln1}, I_{Ln2}, I_{Ln3}) are a combination of the greatest achievable values for the load current, PCC voltage, and nth-order harmonic component phase angle.

$$i_L(t) = \begin{bmatrix} i_{l1} \\ i_{l2} \\ i_{l3} \end{bmatrix} = \begin{bmatrix} \sum_{x=1}^{N} I_{Lx1} \sin(x\omega t - \emptyset_{x1}) \\ \sum_{x=1}^{N} I_{Lx2} \sin(x(\omega t - 120°) - \emptyset_{x2}) \\ \sum_{x=1}^{N} I_{Lx3} \sin(x(\omega t + 120°) - \emptyset_{x3}) \end{bmatrix} \tag{11}$$

$$I^*_{xs1} = \frac{2P_S}{3V_{S1}} \tag{12}$$

$$\begin{aligned} I^{ó*}_{sx1}(t) &= I^*_{xs1} u_{sx} \\ I^{ó*}_{sy}(t) &= I^*_{xs1} u_{sy} \\ I^{ó*}_{sz}(t) &= I^*_{xs1} u_{sz} \end{aligned} \tag{13}$$

$$\begin{aligned} u_{sx}(\Gamma) &= u_a(t) \\ u_{sy}(\Gamma) &= -\frac{1}{2} u_a(t) + \frac{\sqrt{3}}{2} u_b(t) \\ u_{sz}(t) &= -\frac{1}{2} u_a(t) - \frac{\sqrt{3}}{2} u_b(t) \end{aligned} \tag{14}$$

$Vm*$ is the maximum value of the fundamental aspect of the typical maximum voltage, where P is the true power given by the RES and P_L is the true power of the load; hence, I^*_{xs1} is an essential part of the source current element expressed in the preceding equation.

The equations $u_a(t)$ and $u_b(t)$ are used to express the distance between pairs of nearby reference currents. The current inverter and the standard inverter's present errors are provided as input to the Hysteresis current controller (i_{ca}, i_{cb}, i_{cc}), which then applies the resulting equation to change the PWM inverter's duty ratio.

$$\begin{aligned} \Delta i_{ca} &= I * C_1(t) - i_{c1} \\ \Delta i_{cb} &= I * C_2(t) - i_{c2} \\ \Delta i_{cc} &= I * C_3(t) - i_{c3} \end{aligned} \tag{15}$$

The hysteresis regulator, which is based on the disparity between the inverter's true and apparent currents, controls and modulates the pulse in the grid-connected adapter's gate controllers.If i_{c1} is greater than Hb, then S1 is on and S4 is off in inverter phase A, and if i_{c1} is less than Hb, then S1 is on and S4 is off. Each leg will experience switching pulses with the same period. A power electronics conversion and control unit make up the actual filtering process, which generates a compensation current that balances off the harmonic current. A system of control feedback mechanism recognises the harmonic current and enhances the voltage profile in order to determine the amount of compensatory current required.

5. HYBRID SHUNT ACTIVE POWER FILTER SYSTEM

5.1 Importance of hybrid shunt active power filter

HSAPFs are highly effective in mitigating harmonics in electrical systems. Harmonics, which are unwanted electrical frequencies or distortions in the sinusoidal voltage and current waveforms, can lead to a range of problems, including increased equipment stress, malfunctions, and inefficiencies. HSAPFs can filter out these harmonics and provide a cleaner, more stable power supply. HSAPFs can help in reducing voltage sags and swells, which can occur due to rapid changes in load conditions or disturbances in the electrical network [39]. By injecting compensating currents, HSAPFs stabilize the voltage and ensure a more consistent supply to connected loads.

Figure 3 depicts the power circuit and control circuit block diagram that make up a shunt active power filter. The duty of synthesizing the necessary compensatory current falls on the power circuit. The DC voltage is maintained and regulated using a PWM-based voltage source inverter (VSI) and energy is stored in a DC-link capacitor. The power circuit is precisely controlled to synthesis the appropriate harmonic current as the control circuit continually monitors the current's variation and derives the instantaneous reference compensation. In the next section, we will discuss how the efficiency of the harmonic current compensation process may be considerably enhanced by employing harmonic recovery and current regulation methodologies [33]. When the filter is connected at the juncture that has common connection, the system's current flow can be written as follows:

$$i_S = i_L = i_{1L} + i_H \tag{16}$$

where, i_S is the original current, i_L is the load's current, i_{IL} represents the standard load current component and i_H refers to the harmonic portion of the load current.

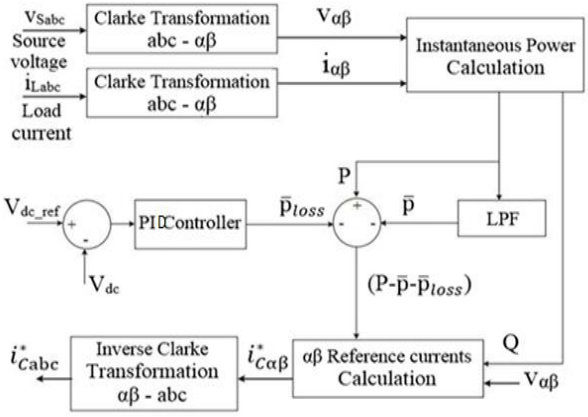

Figure 3. Simplified representations depicting the active and reactive power theories

One is the DC-link current,which is used by the hybrid shunt active power filter to keep the DC-link voltage at the desired level, and the other is the harmonic compensation current (Ihc), which is the same magnitude as the harmonic current but has a phase shift of 180 degrees. Both currents appear after the designed filter.

$$i_S = i_L = [i_{1L} + i_H] - i_C + i_{dc} \tag{17}$$

$$i_S = i_{1L} + i_{dc} \tag{18}$$

5.2 Importance of Clarke transformations in the proposed model

The efficacy of a shunt active power filter can be influenced by harmonic extraction estimations. The instantaneous reactive power theory relies on the Clarke transformation, which maps the a-b-c reference coordinate of a stationary frame of reference to the rotary frame of reference. Take a look at this formula to get a better idea of how the voltages and currents at the source are transformed into the succeeding variables.

$$\begin{bmatrix} v_0 \\ v_\alpha \\ v_\beta \end{bmatrix} = \sqrt{\frac{2}{3}} \begin{bmatrix} 1/\sqrt{2} & 1/\sqrt{2} & 1/\sqrt{2} \\ 1 & -1/2 & -1/2 \\ 0 & \sqrt{3}/2 & \sqrt{3}/2 \end{bmatrix} . \begin{bmatrix} v_a \\ v_b \\ v_c \end{bmatrix} \tag{19}$$

$$\begin{bmatrix} i_0 \\ i_\alpha \\ i_\beta \end{bmatrix} = \sqrt{\frac{2}{3}} \begin{bmatrix} 1/\sqrt{2} & 1/\sqrt{2} & 1/\sqrt{2} \\ 1 & -1/2 & -1/2 \\ 0 & \sqrt{3}/2 & \sqrt{3}/2 \end{bmatrix} . \begin{bmatrix} i_a \\ i_b \\ i_c \end{bmatrix} \tag{20}$$

In two axes coordinate, P and Q constitute an intricate sum of active and reactive powers.

$$S = P + jQ = v_{\alpha\beta} i^*_{\alpha\beta} = (v_\alpha - jv_\beta)(i_\alpha + ji_\beta) \tag{21}$$

5.3 Determining PID controller's parameters

A proportional-integral derivative regulator regulates harmonic current and preserves DC-link voltage in the control loop.

PID controller's transfer function is given by:

$$C(s) = k_p + \frac{k_i}{s} + sk_d \tag{22}$$

where, k_p is the proportional increment, k_i is the integral increment and k_d is the derivative increment.

This is the result from the PID controller use in the power system.

$$u_{1,2} = k_{p1} vd_{1,2} + k_i \int_0^T vd_{1,2} dt + \frac{dvd_{1,2}}{dt} \tag{23}$$

$$u_{1,2} = k_{p1} vh_{1,2} + k_i \int_0^T vh_{1,2} dt + \frac{dvh_{1,2}}{dt} \tag{24}$$

Using information about the voltage and its harmonics, such as the performance index ITAE, the PID controller's gain is adjusted such that the steady-state error is as small as possible.

$$J = ITAE = \int_0^t u_{1,2} dt \tag{25}$$

where, the error is analyzed based on the objective function.

Intelligence optimisation algorithms approaches and the proposed novel method can be used to fine-tune the values of the PID controller's parameters.

6. RECOMMENDED OPTIMIZATION TECHNIQUE

To fine-tune the PID controller settings of a hybrid microgrid system, an innovative hybrid metaheuristic optimization is developed that takes the best aspects of swarm-inspired algorithms like sparrow search optimization and Gray wolf optimization.

6.1 Gray wolf optimization

One widespread swarm optimisation approach is Gray wolf optimization. The application, which is inspired by the tracking, enclosing, and hunting behaviours of the grey wolf population, searches and optimises in a manner similar to these natural behaviours.

Based on their relative levels of authority within the pack, wolves can be classified as α, β, δ, and w . In a created group if w is the pathfinder then α, β, δ are the top three options for the problem. The gray wolves must work together as a group in order to be successful. The strategy entails encircling and attacking the prey.

6.1.1 Encircling the prey

During a hunt, gray wolves frequently huddle around their prey. To replicate encirclement by gray wolves, we can use:

$$\vec{D} = \left| \vec{C} \cdot \vec{X}_P(t) - X(t) \right| \tag{26}$$

$$\vec{X}(t+1) = \vec{X_P}(t) - \vec{A} \cdot \vec{D} \tag{27}$$

$\vec{A}$ and $\vec{C}$ can be formulated as follows:

$$\vec{A} = 2\vec{a} \cdot \vec{r_1} - \vec{a} \tag{28}$$

$$\vec{C} = 2 \cdot \vec{r_2} \tag{29}$$

Over the course of all possible iterations, the value of $\overrightarrow{a}$ goes from 2 to 0 in a linear fashion. $\overrightarrow{r_1}$ and $\overrightarrow{r_2}$ are randomly generated vectors.

6.1.2 Gray wolf tracking technique

Because they are more capable of anticipating where the target is going to be, the alphas, betas, and deltas typically take the lead in the chase. The other mediators in the preliminary process will have to readjust to the new hierarchy established by the best mediator.

$$\left.\begin{array}{c} \vec{D}\alpha 1 = \left|\vec{C} \cdot \overrightarrow{X_{\alpha 1}} - \vec{X}\right| \\ \vec{D}\beta 1 = \left|\vec{C} \cdot \overrightarrow{X_{\beta 1}} - \vec{X}\right| \\ \overrightarrow{D_{\delta}} = \left|\vec{C} \cdot \overrightarrow{X}_{\delta} - \vec{X}\right| \\ \vec{X}1 = \overrightarrow{X}\alpha - \overrightarrow{A}1.\vec{D}\alpha \\ \overrightarrow{X}2 = \vec{X}\beta - \overrightarrow{A}2.\vec{D}\beta; \\ \vec{X}3 = \overrightarrow{X}\delta - \overrightarrow{A}3.\vec{D}\delta \\ \vec{X}(t+1) = \dfrac{\overrightarrow{X_1} + \overrightarrow{X_2} + \overrightarrow{X_3}}{3} \end{array}\right\} \quad (30)$$

Since the alpha wolf leads the pack and probably knows where the target is, that seems to be the most probable assumption. In this repetition, the β wolf is the second-best choice and the δ wolf is the third-best choice. A is the arbitrary integer. Use of random integer A causes the wolves to abandon the kill.Moreover, the wolves are compelled to separate from the prey (local minimum) when the value of |A|>1.

6.2 Sparrow search optimization

This method imitates the foraging behaviour of sparrows. It exhibits three distinct behavioural types: investigator, follower, and discoverer. The sparrows also update their locations in accordance with their own set of rules. The explorer finds food and leads the other members of the society. Following their discovery of the discoverer's location, followers look for food in the area.

The exact position can be modified using the formula below:

$$X_i^{t+1} = \left\{\begin{array}{ll} Q \cdot e^{\left(\frac{X_{worst} - X_i^t}{I^2}\right)}, & i > \dfrac{n}{2} \\ X_{best}^{t+1} + |X_i^t - X_{best}^{t+1}| \cdot A \cdot L, & i \le \dfrac{n}{2} \end{array}\right\} \quad (31)$$

where, A is a matrix with d rows and d columns ,where n is the total quantity of sparrows, X_{best} represents each bird's optimal position at this time, and 1 or -1 is allocated at random to all other factors.The current lowest place is called X_{worst}. If i>n/2, it indicates that the ith entrant must take a plane to a different location in order to find food; if i<n/2, then the ith contestant is probably trying to find some aliment in or around the best possible spot.

A random sample of individuals is selected to act as monitors. When threatened, sparrows send out alarm calls that encourage other birds to seek refuge nearby.

Accuracy and speed of convergence in SSA are directly impacted by the mutation approach. The SSA has lower population diversity and less accurate convergence, but it performs better when addressing complicated optimization problems. It can fail to find the best solution to the issues and instead settle into the local optimum.

6.3 Proposed grey wolf supported sparrow search optimization algorithm

This paper proposes GWSSSOA, an improved version of the GWO-inspired hybrid sparrow search algorithm. Because of its characteristics, the GWSSSOA can improve convergence speed and accuracy without reaching the local optimum. To enhance its exploitation potential, the sparrow search algorithm incorporates the GWO's exploitation capacity.By incorporating the exploratory behaviour of GWO into the revised framework of SSA, we are able to strike a balance between the two, hence enhancing the exploitation capability as shown in Table 5. Hybridization between SSA and GWO is needed for improving exploitation in SSA along with exploration and the proposed algorithm parameters are shown in Table 6. Importance of proposed algorithm can be understood from below:

Table 5. Advantages of proposed system

Performance Parameter	GWO	SSO	Hybrid GWSSSOA
No of parameters	less	Maximum iteration	less
Convergence speed	slow	fast	fast
Accuracy	low	high	high

To maintain solutions to the problem close to their optimal values, we combine the versions of position from SSA Eq. (32) by utilising a modified scale in the GWO proximity calculation. The suggested procedure is based on the stages shown in Figure 4. Following is a restatement of the equations based on the changes made:

$$\begin{array}{l} \overrightarrow{D_{\alpha}} = \left|\overrightarrow{C_1} \cdot \overrightarrow{X_{\alpha}} - \theta\vec{X}\right| \\ \overrightarrow{D_{\beta}} = \left|\overrightarrow{C_1} \cdot \overrightarrow{X_{\beta}} - \theta\vec{X}\right|, \\ \overrightarrow{D_{\delta}} = \left|\overrightarrow{C_1} \cdot \overrightarrow{X_{\delta}} - \theta\vec{X}\right| \end{array} \quad (32)$$

Using below Eq. (33) we may determine the likelihood of a global relocation of all agents.

$$\Gamma|X(t+1) - X(t)| = \left|\frac{X(t+1) - X(t)}{\sqrt{[X(t+1) - X(t)]^2 + 1}}\right| \quad (33)$$

where, Γ is the probability.

The sparrows choose the sustenance if the outcome of Eq. (33) is positive, and they avoid intruders if the result is negative.It is important to note that by carefully choosing the limits of the PID variables, the desired position can be attained rapidly and updated in Eq. (34):

$$X_i^{t+1} = \left\{\begin{array}{ll} X_{best}^t + \beta|X_i^t - X_{best}^{t+1}|, & v > v_{target} \\ X_{best}^{t+1} + K\frac{X_i^t - X_{best}^{t+1}}{(vi - vn) + e}, & v = v_{target} \end{array}\right\} \quad (34)$$

Table 6. Parameters of proposed algorithm

S.No	Parameters	Values
1	Maximum iteration	100
2	Number of search agents	50
3	% of total population	0.2

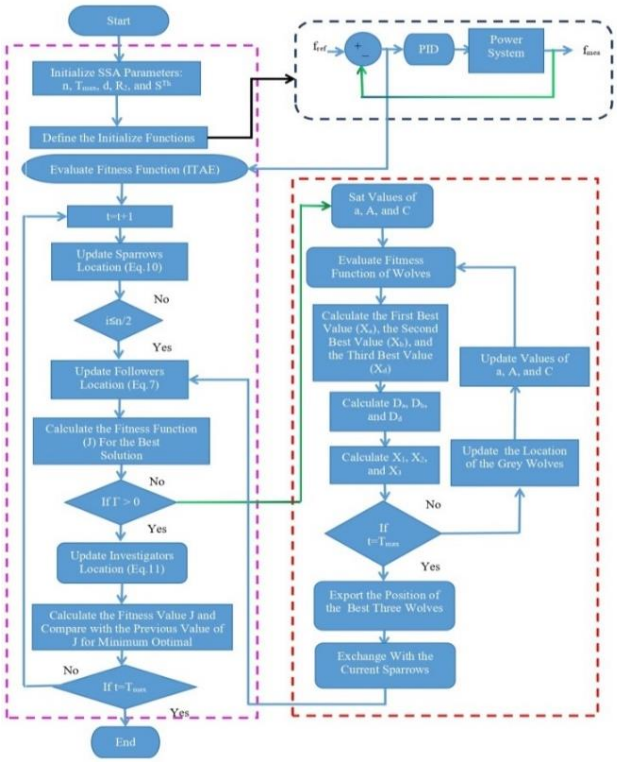

Figure 4. Process diagram for the developed hybrid algorithm

7. EVALUATION AND SIMULATION RESULTS

As a first step, the effectiveness of GWSSSOA is compared to that of SSA and GWO. Under the impact of nonlinear load and sag/swell of the voltage, MATLAB/Simulink has been used to examine voltage regulation and distortion caused by harmonics.

Figures 5(a) and (b) show the source voltage and source current of the a-phase prior to adjustment. To illustrate the dynamic behaviour under abrupt changes in load, by introducing another load at [t=0.1s]. It's easy to see that after applying the control, the grid current takes on a perfectly sinusoidal shape; in fact, it's in this momentary stage that the goal of achieving unity power factor is realized.

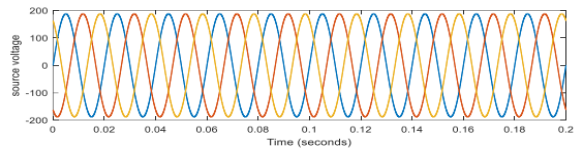

(a) Variation of source voltage

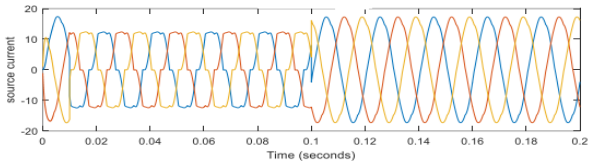

(b) Variation of source current

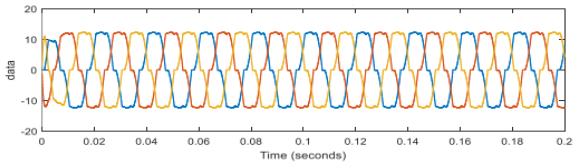

(c) Change in current w.r.t load

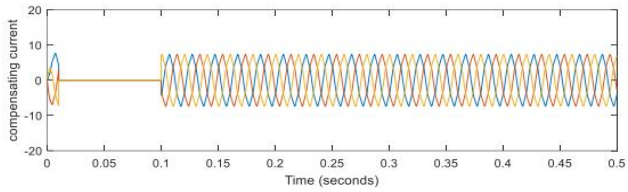

(d) Variation of balancing current

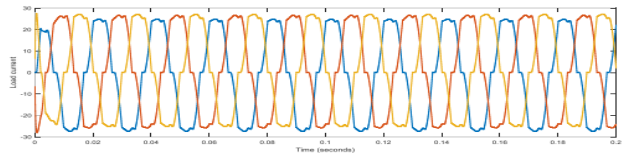

(e) Variation of load current with controller

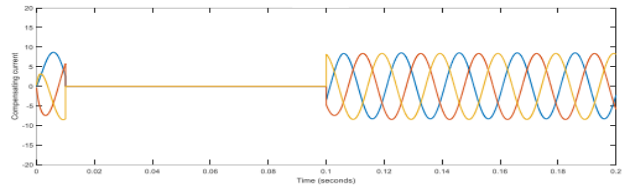

(f) Variation of compensating current with controller

Figure 5. Different results with nonlinear load and without controller

Table 7. Parameters of system

Parameters	Value
Source voltage (Vrms)	220V
The impedance of source Rs, Ls	3mΩ, 2.6μH
frequency of switching	12kHz
impedances of series filter(R,L,C)	1.5Ω,3mH, 0.1mF
impedances of line (R,L,)	10.0mΩ, 0.3μH
Diode rectifier load(Rd,Ld)	15.0Ω, 2mH
reference of DC-link voltage	900V
Boost converter	5mH, 55mF
impedances of components in filter (R,L,C)	20mΩ, 2.5mH

Table 7 lists all of the specified values for the system.

Modifications in source voltage, source current, and load current are shown in Figure 5(b), (c), and (d), with distorted source current evident between (0.01 and 0.1) sec and demand-induced distortion becoming less evident between 0 and 0.2 sec. The compensator is operational throughout the operating period, but particularly during the intervals (0.01 and 0.1) characterized by dynamic variations. Table 8 compare the suggested method's optimal gain value with the values obtained using different approaches that have previously been used in the literature. Table 8 shows how effective the tuned parameters using the proposed GWSSSOA approach are.

Case a: Base case condition

Voltage and current dispersion due to harmonics are measured at separate buses in the aforementioned standard instance. The nonlinear load is connected to terminal 14 on bus 14. Here, we evaluate the performance of both traditional PID and GWSSSOA based PID controllers. PID controller gains are shown in Table 8. Bus 7 is experiencing an instance of uneven loading. Both the arc furnace on bus 9 and the diode bridge rectifier on bus 10 are candidates for investigation. The base case variations are shown in Table 9.

Results for the GWSSSOA based PID parameters' voltage responses are displayed, with voltage regulation improvement being another important parameter of this work. Tables 10 and

11 display stability indices that can be used to pinpoint problematic bus routes.

Table 8. Relative PID controller strengths

Method	Kp	Ki
DE [40]	5.0843	9.7187
ABC [40]	8.2655	3.6173
HS [40]	9.1285	3.5781
PSO [40]	7.2105	3.6122
GWO [40]	4.8705	9.9654
GWSSSOA	2.9812	4.7698

Table 9. PID+GWSSSOA optimal base case conditions for control variables

Control Variables	Bus Number	Base Case		
		PID	PID+ GWSSSOA	% Decrease in THD
V_H(%)	14	3.8	2.7	28.94
	7	4.5	3.6	20
	10	6.8	5.2	23.52
	9	8.7	4.5	48.27
I_H(%)	14	4.6	3.7	19.56
	7	5.2	4.9	5.76
	10	7.1	6.8	4.2
	9	8.9	7.2	19.10

Table 10. Voltage stability index for prioritising critical buses

No	Observed Value	Simplified Index(SVSI)	Ranking
3	**1.005**	**0.8271**	**1**
7	0.9722	0.7421	2
6	0.9643	0.4374	3
8	1.015	0.2707	4
5	1.0063	0.2291	**5**
4	**0.9758**	**0.1488**	6
10	1.0091	0.1367	**7**
1	**0.8955**	**0.1229**	8
9	0.8889	0.0936	9
14	0.9787	0.0803	10
11	0.8995	0.0788	11
12	0.8889	0.0693	**12**
2	0.8889	0.0693	**13**
13	0.8889	0.0693	**14**

Table 11. Voltage stability indices at various buses

Bus No	Voltage Harmonic Distortion (%)	Voltage Sag Rank	Voltage Imbalance
2	3.6	0.14	0.05
4	4.8	0.22	0.1
5	2.32	0.3	1.1
6	6.91	1.45	1.0
7	2.24	**0.2**	**1.01**
8	4.17	0.15	1.1
9	5.25	**0.43**	**1.07**
10	2.12	0.31	-
11	7.07	0.18	0.5
12	8.49	0.64	0.1
13	3.76	0.52	1.04
14	2.33	**0.12**	**0.3**

Voltage stability index analysis, through the ranking of buses, contributes to the overall resilience of the grid. It helps in identifying vulnerabilities and weak points, allowing for better planning and preparedness in the face of contingencies, such as generator outages or faults.

The recommended controller's efficacy is tested in MATLAB/Simulink. The effects of GWSSSOA controller on two distinct loads are analyzed.

Case b: Load performance with GWSSSOA controller

Table 11 shows that the voltage fluctuations in the selected microgrid are reduced using the GWSSSOA based controller as compared to the PSO+PID based other optimum controller. It's also worth noting that GWSSSOA -based PID controllers can significantly boost system performance. Due to its low-frequency variation and short transitory variation, the data show that GWSSSOA excels over PSO+PID. The quality of the voltage is quantified by how far the real voltage is from the ideal voltage. Various buses in the chosen system can have their voltage quality evaluated using voltage quality indicators.

We apply a random step change in load demand to designed system to analyze the performance of the suggested algorithm. Table 12 depicts the change of harmonics due to change of various controllers. The results showed that in comparison to other optimization methods, the suggested approach quickly optimizes the PID controller's reaction to a sudden change in load. With the increase in fundamental component the active power loss can be diminished.

Table 12. Assessing the THD for different controllers

Controller	THD	Different Harmonic Components as a % of Fundamental	
PID	7.97	**Harmonic Order**	PID
		3rd	
		5th	
		7th	
		9th	
		11th	
		13th	
		15th	
		17th	
PID+PSO	3.97	**Harmonic Order**	PID+PSO
		3rd	
		5th	
		7th	
		9th	
		11th	
		13th	
		15th	
		17th	
PID+ GWSSSOA	2.95	**Harmonic Order**	PID+ GWSSSOA
		3rd	
		5th	
		7th	
		9th	
		11th	
		13th	
		15th	
		17th	

8. CONCLUSIONS

By evaluating the voltage quality,and harmonic distortion, the selected hybrid optimization based controller was shown to be the most effective. The best place to put loads and maximize system efficiency is determined by the voltage quality indices measured at each bus. To assess the quality of the voltage and identify the prevailing harmonic at extremely important buses, reactive power is computed in response to a percentage shift in load. In conclusion, the microgrid voltage control is very amenable to the optimization technique chosen for being based on the control strategy. Future evaluations of the system's performance in terms of additional power quality phenomena may make use of the chosen controller.

ACKNOWLEDGMENT

The authors are thankful to the administration of Annamalai University for allowing them to utilise the university's facilities to complete their research.

REFERENCES

[1] Shezan, S.A., Kamwa, I., Ishraque, M.F., Muyeen, S.M., Hasan, K.N., Saidur, R., Rizvi, S.M., Shafiullah, M., Al-Sulaiman, F.A. (2023). Evaluation of different optimization techniques and control strategies of hybrid microgrid: A review. Energies, 16(4): 1792. https://doi.org/10.3390/en16041792

[2] Thirunavukkarasu, G.S., Seyedmahmoudian, M., Jamei, E., Horan, B., Mekhilef, S., Stojcevski, A. (2022). Role of optimization techniques in microgrid energy management systems—A review. Energy Strategy Reviews, 43: 100899. https://doi.org/10.1016/j.esr.2022.100899

[3] Sindi, H.F., Alghamdi, S., Rawa, M., Omar, A.I., Elmetwaly, A.H. (2023). Robust control of adaptive power quality compensator in Multi-Microgrids for power quality enhancement using puzzle optimization algorithm. Ain Shams Engineering Journal, 14(8): 102047. https://doi.org/10.1016/j.asej.2022.102047

[4] Palanisamy, R., Govindaraj, V., Siddhan, S., Albert, J.R. (2022). Experimental investigation and comparative harmonic optimization of AMLI incorporate modified genetic algorithm using for power quality improvement. Journal of Intelligent & Fuzzy Systems, 43(1): 1163-1176.

[5] Leonori, S., Paschero, M., Mascioli, F.M.F., Rizzi, A. (2020). Optimization strategies for Microgrid energy management systems by Genetic Algorithms. Applied Soft Computing, 86: 105903. https://doi.org/10.1016/j.asoc.2019.105903

[6] Zhang, X., Lin, Q., Mao, W., Liu, S., Dou, Z., Liu, G. (2021). Hybrid particle swarm and grey wolf optimizer and its application to clustering optimization. Applied Soft Computing, 101: 107061. https://doi.org/10.1016/j.asoc.2020.107061

[7] Fadheel, B.A., Wahab, N.I.A., Mahdi, A.J., Premkumar, M., Radzi, M.A.B.M., Soh, A.B.C., Veerasamy, V., Irudayaraj, A.X.R. (2023). A hybrid grey wolf assisted-sparrow search algorithm for frequency control of re integrated system. Energies, 16(3): 1177. https://doi.org/10.3390/en16031177

[8] Nakiganda, A.M., Van Cutsem, T., Aristidou, P. (2021). Microgrid operational optimization with dynamic voltage security constraints. In 2021 IEEE Madrid PowerTech, Madrid, Spain, pp. 1-6. https://doi.org/10.1109/PowerTech46648.2021.9494823

[9] Mansoorhoseini, P., Mozafari, B., Mohammadi, S. (2022). Islanded AC/DC microgrids supervisory control: A novel stochastic optimization approach. Electric Power Systems Research, 209: 108028. https://doi.org/10.1016/j.epsr.2022.108028

[10] Xue, J., Shen, B. (2020). A novel swarm intelligence optimization approach: Sparrow search algorithm. Systems Science & Control Engineering, 8(1): 22-34. https://doi.org/10.1080/21642583.2019.1708830

[11] Azimi, A., Hashemi-Dezaki, H. (2023). Optimized protection coordination of microgrids considering power quality-based voltage indices incorporating optimal sizing and placement of fault current limiters. Sustainable Cities and Society, 96: 104634. https://doi.org/10.1016/j.scs.2023.104634

[12] Nakka, S., Brinda, R., Sairama, T. (2023). Design and simulation of monarch butterfly optimized SP-UPFC for power quality compensation. Computers and Electrical Engineering, 110: 108800. https://doi.org/10.1016/j.compeleceng.2023.108800

[13] Fu, L., Deng, X., Chai, H., Ma, Z., Xu, F., Zhu, T. (2023). PQEventCog: Classification of power quality disturbances based on optimized S-transform and CNNs with noisy labeled datasets. Electric Power Systems Research, 220: 109369. https://doi.org/10.1016/j.epsr.2023.109369

[14] Sahoo, G.K., Choudhury, S., Rathore, R.S., Bajaj, M. (2023). A novel prairie dog-based meta-heuristic optimization algorithm for improved control, better transient response, and power quality enhancement of hybrid microgrids. Sensors, 23(13): 5973. https://doi.org/10.3390/s23135973

[15] Singh, N., Ansari, M.A., Tripathy, M., Gupta, P., Ali, I., Rawea, A.S. (2023). Enhancing the hybrid microgrid performance with jellyfish optimization for efficient MPPT and THD estimation by the unscented kalman filter. International Transactions on Electrical Energy Systems, 2023: 5661381. https://doi.org/10.1155/2023/5661381

[16] Han, Y., Feng, Y., Yang, P., Xu, L., Xu, Y., Blaabjerg, F. (2019). Cause, classification of voltage sag, and voltage sag emulators and applications: A comprehensive overview. IEEE Access, 8: 1922-1934. https://doi.org/10.1109/ACCESS.2019.2958965

[17] Nagata, E.A., Ferreira, D.D., Bollen, M.H., Barbosa, B.H., Ribeiro, E.G., Duque, C.A., Ribeiro, P.F. (2020). Real-time voltage sag detection and classification for power quality diagnostics. Measurement, 164: 108097. https://doi.org/10.1016/j.measurement.2020.108097

[18] Caicedo, J.E., Agudelo-Martínez, D., Rivas-Trujillo, E., Meyer, J. (2023). A systematic review of real-time detection and classification of power quality disturbances. Protection and Control of Modern Power Systems, 8(1): 3. https://doi.org/10.1186/s41601-023-00277-y

[19] Vinayagam, A., Othman, M.L., Veerasamy, V., Saravan Balaji, S., Ramaiyan, K., Radhakrishnan, Abdul Wahab, N.I. (2022). A random subspace ensemble classification model for discrimination of power quality events in solar PV microgrid power network. PloS One, 17(1):

e0262570. https://doi.org/10.1371/journal.pone.0262570
[20] Lawal, M.J., Hussein, S.U., Saka, B., Abubakar, S.U., Attah, I.S. (2023). Intelligent fuzzy-based automatic voltage regulator with hybrid optimization learning method. Scientific African, 19: e01573. https://doi.org/10.1016/j.sciaf.2023.e01573
[21] Beza, T.M., Huang, Y.C., Kuo, C.C. (2020). A hybrid optimization approach for power loss reduction and DG penetration level increment in electrical distribution network. Energies, 13(22): 6008. https://doi.org/10.3390/en13226008
[22] Kansit, S., Assawinchaichote, W. (2016). Optimization of PID controller based on PSOGSA for an automatic voltage regulator system. Procedia Computer Science, 86: 87-90. https://doi.org/10.1016/j.procs.2016.05.022
[23] Mitra, P., Maulik, S., Chowdhury, S.P., Chowdhury, S. (2007). ANFIS based automatic voltage regulator with hybrid learning algorithm. In 2007 42nd International Universities Power Engineering Conference, pp. 397-401. https://doi.org/10.1109/UPEC.2007.4468980
[24] Yang, Z., Wang, C., Han, J., Yang, F., Shen, Y., Min, H., Hu, W., Song, H. (2023). Analysis of voltage control strategies for DC microgrid with multiple types of energy storage systems. Electronics, 12(7): 1661 https://doi.org/10.3390/electronics12071661
[25] Kumar, S., Kumar, A. (2023). Ant lion optimized hybrid-fuzzy-PID controller for frequency-voltage regulation in hybrid power system. International Journal of Computing and Digital Systems, 13(1): 1-1.
[26] Ullah, Z., Wang, S., Lai, J., Azam, M., Badshah, F., Wu, G., Elkadeem, M.R. (2023). Implementation of various control methods for the efficient energy management in hybrid microgrid system. Ain Shams Engineering Journal, 14(5): 101961 https://doi.org/10.1016/j.asej.2022.101961
[27] Dashtdar, M., Flah, A., Hosseinimoghadam, S.M.S., Reddy, C.R., Kotb, H., AboRas, K.M., Bortoni, E.C. (2022). Improving the power quality of island microgrid with voltage and frequency control based on a hybrid genetic algorithm and PSO. IEEE Access, 10: 105352-105365. https://doi.org/10.1109/ACCESS.2022.3201819
[28] Hou, X., Sun, K., Zhang, N., Teng, F., Zhang, X., Green, T.C. (2021). Priority-driven self-optimizing power control scheme for interlinking converters of hybrid AC/DC microgrid clusters in decentralized manner. IEEE Transactions on Power Electronics, 37(5): 5970-5983. https://doi.org/10.1109/TPEL.2021.3130112
[29] Espina, E., Cárdenas-Dobson, R., Simpson-Porco, J.W., Kazerani, M., Sáez, D. (2023). A consensus-based distributed secondary control optimization strategy for hybrid microgrids. IEEE Transactions on SmartGrid. https://doi.org/10.1109/TSG.2023.3263107
[30] Salah, B., Hasanien, H.M., Ghali, F.M., Alsayed, Y.M., Abdel Aleem, S.H., El-Shahat, A. (2022). African vulture optimization-based optimal control strategy for voltage control of islanded DC microgrids. Sustainability, 14(19): 11800. https://doi.org/10.3390/su141911800
[31] Shuai, Z., Fang, J., Ning, F., Shen, Z.J. (2018). Hierarchical structure and bus voltage control of DC microgrid. Renewable and Sustainable Energy Reviews, 82: 3670-3682. https://doi.org/10.1016/j.rser.2017.10.096
[32] Rajesh, P., Shajin, F.H., Rajani, B., Sharma, D. (2022). An optimal hybrid control scheme to achieve power quality enhancement in micro grid connected system. International Journal of Numerical Modelling: Electronic Networks, Devices and Fields, 35(6): e3019. https://doi.org/10.1002/jnm.3019
[33] Ostrowska, A., Michalec, Ł., Skarupski, M., Jasiński, M., Sikorski, T., Kostyła, P., Lis, R., Mudrak, G., Rodziewicz, T. (2022). Power quality assessment in a real microgrid-statistical assessment of different long-term working conditions. Energies, 15(21): 8089. https://doi.org/10.3390/en15218089
[34] Kumar, R. (2022). Fuzzy particle swarm optimization control algorithm implementation in photovoltaic integrated shunt active power filter for power quality improvement using hardware-in-the-loop. Sustainable Energy Technologies and Assessments, 50: 101820. https://doi.org/10.1016/j.seta.2021.101820
[35] Singh, M., Chauhan, S. (2023). A hybrid-extreme learning machine based ensemble method for online dynamic security assessment of power systems. Electric Power Systems Research, 214: 108923. https://doi.org/10.1016/j.epsr.2022.108923
[36] Sathish Babu, P., Sundarabalan, C.K., Balasundar, C. (2022). SOFC-Supported hybrid PSOGSA-Optimized dynamic voltage restorer for power quality enhancement. Journal of Circuits, Systems and Computers, 31(01): 2250006. https://doi.org/10.1142/S0218126622500062
[37] Amir, M., Prajapati, A.K., Refaat, S.S. (2022). Dynamic performance evaluation of grid-connected hybrid renewable energy-based power generation for stability and power quality enhancement in smart grid. Frontiers in Energy Research, 10: 861282. https://doi.org/10.3389/fenrg.2022.861282
[38] Arulkumar, T., Chandrasekaran, N. (2022). Development of improved sparrow search-based PI controller for power quality enhancement using UPQC integrated with medical devices. Engineering Applications of Artificial Intelligence, 116: 105444. https://doi.org/10.1016/j.engappai.2022.105444
[39] Imam, A.A., Sreerama Kumar, R., Al-Turki, Y.A. (2020). Modeling and simulation of a PI controlled shunt active power filter for power quality enhancement based on PQ theory. Electronics, 9(4): 637. https://doi.org/10.3390/electronics9040637
[40] Motukuri, D.R., Prakash, P., Rao, M.V.G. (2023). A novel optimization-based approach for harmonic assessment in hybrid microgrids. Journal of Theoretical and Applied Information Technology, 101(16).

NOMENCLATURE

Xp	Xrelated to the parallel filter
Xs	Xrelated to the series filter
P,Q	P Q Active Power (W) Reactive Power (VAR)
THD	Total Harmonic Distortion
V_H	Voltage harmonic
I_H	Current harmonic